Lamellae orientation in dynamically sheared diblock copolymer melts

Kurt Koppi, Matthew Tirrell, Frank Bates, Kristoffer Almdal, Ralph Colby

J. Phys. II France **2** (1992) 1941-1959 NOVEMBER **1992**, PAGE 1941

Classification
Physics Abstracts
61.41 — 61.25H — 81.30

Lamellae orientation in dynamically sheared diblock copolymer melts

Kurt A. Koppi ([1]), Matthew Tirrell ([1]), Frank S. Bates ([1]) Kristoffer Almdal ([2]) and Ralph H. Colby ([3])

([1]) Department of Chemical Engineering and Materials Science, University of Minnesota, Minneapolis, MN 55455, U.S.A.
([2]) Risø National Laboratory, Roskilde, Denmark
([3]) Corporate Research Laboratories, Eastman Kodak Company, Rochester, NY 14650-2110, U.S.A.

(Received 13 May 1992, accepted 5 august 1992)

Résumé . — Nous avons identifié, par diffusion de neutrons aux petits angles, deux orientation différentes des lamelles dans des échantillons de copolymères séquencés poly(éthylène-propylène)- poly(éthyléthylène) (PEP-PEE) qui ont été cisaillés dynamiquement. A des températures proches de la transition ordre-désordre et aux fréquences de cisaillement faibles, la normale aux couches est perpendiculaire à la direction d'écoulement et parallèle au gradient de vitesse (orientation parallèle). Aux fréquences plus élevées, la normale est perpendiculaire à la direction d'écoulement et au gradient de vitesse (orientation perpendiculaire). Le changement d'orientation survient pour des fréquences de l'ordre de l'inverse du temps de relaxation des déformations locales des domaines ordonnés. Aux températures très inférieures à la transition ordre-désordre, l'orientation est parallèle à toutes les fréquences de cisaillement. En tenant compte des mesures rhéologiques, on propose deux mécanismes. Dans l'orientation perpendiculaire, le système est d'abord désordonné par le cisaillement puis s'oriente grâce aux effets de vorticité. L'orientation parallèle résulte de la relaxation des contraintes en présence de défauts. Ces hypothèses sont confirmées par des expériences de cisaillement sur une gamme d'échantillons variés de copolymères bi-séquencés de structures différentes.

Abstract . — Two distinct lamellae orientations have been identified by small-angle neutron scattering (SANS) in dynamically sheared poly(ethylene-propylene)-poly(ethylethylene) (PEP-PEE) diblock copolymer melts. Near the order-disorder transition temperature, $T \rightarrow T_{ODT}$, and at low shear frequencies, the lamellae arrange with unit normal perpendicular to the flow direction and parallel to the velocity gradient direction (parallel orientation). Higher frequency processing leads to lamellae with unit normal perpendicular to both the flow and velocity gradient directions (perpendicular orientation). The crossover from low to high frequency behavior occurs at $\omega \approx \tau^{-1}$ where τ is the relaxation time for local domain deformations. At temperatures further from the ODT, $T << T_{ODT}$, the parallel orientation is obtained at all shearing frequencies. Based on dynamic and steady shear rheological measurements we propose two

mechanisms to account for these results. The perpendicular orientation is proposed to arise from shear-induced disordering, followed by reordering in the perpendicular direction due to the effect of vorticity. Parallel lamellae are believed to be a manifestation of defect mediated stress relaxation. These findings are supported by additional experiments on various other shear-oriented polyolefin diblock copolymers.

1. Introduction.

Deformation-driven changes in the structure and properties of ordered condensed matter are of central importance to the development of new materials. Our understanding of the processes responsible for the creation of strain through an applied stress is most developed for "hard" substances such as metals. The physical properties of "soft" ordered materials, including liquid crystals, microemulsions, colloids, and block copolymers are less easily correlated with their unperturbed structural features. One reason for this is that, owing to the ease with which defects are created thermally and mechanically, "soft" materials are seldom observed in an ordered state that is coherent on macroscopic length scales. And in general, these substances are highly susceptable to flow fields, leading to microstructural rearrangements that may involve symmetry breaking phase transitions.

Ordered block copolymer melts are exceptionally well-suited for investigating such phenomena. Microstructural size and symmetry can be controlled through the copolymer molecular weight and composition, respectively [1]. Owing to the intrinsically long relaxation times of polymer melts, the deformation rate can be easily varied so that either short-range (e.g., entanglement) or long-range (e.g., microstructural) modes are excited [2]. Furthermore, by adjusting the overall molecular weight, specimens can be placed in either an ordered or disordered state at a convenient temperature [1].

Flow induced orientation of block copolymer melt microstructures was discovered over two decades ago by Keller *et al.* [3]. Extruded plugs of a styrene-butadiene-styrene (SBS) triblock copolymer were found to possess hexagonally packed cylindrical microdomains that were highly aligned with the extrusion direction. These "single-domain" specimens were also characterized by dramatically anisotropic viscoelastic properties [4]. Several years later Terrisse [5] investigated the effects of oscillatory shearing on styrene-isoprene-styrene (SIS) triblock copolymer melts using a Couette device, and concluded that above a certain frequency long-range order is destroyed. Orientation of both triblock (SIS) and diblock (SI) copolymers was later accomplished by Hadziioannou *et al.* [6-8] using a rectalinear shearing apparatus that employed a linear oscillatory shear strain. This design facilitated the removal of shear-oriented samples for subsequent mechanical and small-angle scattering analysis. Hadziioannou *et al.*[6-8] found that dynamically shearing macroscopic specimens containing cylindrical and lamellar microstructures produced highly anisotropic morphologies, with the cylindrical axes aligned with the direction of shear, and the lamellae arranged parallel to the plane of shear. More recently, flow induced orientation has been applied to the study of colloids [9, 10], microemulsions and micellar solutions [11], and liquid crystals [12] and there is currently a renewed interest in the area of block copolymers [13].

Recently, we have been exploring the phase behavior of poly(ethylene-propylene)-poly(ethylethylene) (PEP-PEE) diblock copolymers near the order-disorder transition (ODT) [2, 14-18]. In order to facilitate the identification of new ordered phases, and order-order

transitions, we have built a dynamic shearing device similar to that used by Hadziioannou *et al.* [6-8]. We show here that shear orientation is more than a useful tool in the study of phase transitions. It manifests interesting new physics of its own. Surprisingly, two distinct lamellar orientations have been observed among a variety of specimens studied: the lamallae unit normal perpendicular to the flow direction and parallel to the velocity gradient direction [14], and perpendicular to both the flow and velocity gradient directions [16]. In this paper we examine this behavior using rheological and small-angle neutron scattering experiments. Two distinct mechanisms are proposed to account for these results. These findings also make contact with recent experiments [12] and theory [19] involving sheared lyotropic and thermotropic liquid crystalline materials.

This paper is organized as follows. In section 2 we describe the experimental procedures used in preparing shear-oriented block copolymer specimens for small-angle neutron scattering (SANS) and rheological measurements. The results of the SANS and rheology experiments are presented and analyzed in section 3. Section 4 contains a discussion of our findings including a presentation of tentative mechanisms for the orientation effects observed, and a comparison with recent theory and experiments dealing with liquid crystals. Our results are summarized in section 5.

2. Experimental.

Two PEP-PEE polymers containing 55 % by volume PEP were used in this study. Both were obtained by saturating 1,4-polyisoprene-1,2-polybutadiene diblock copolymers using deuterium gas and a calcium-carbonate-supported palladium catalyst. We have found that this reaction is accompanied by a greater degree of deuterium exchange on the PEP block leading to a modest level of neutron contrast. The synthesis and characterization of the hydrogenated versions of these samples, PEP-PEE-2 and PEP-PEE-3, have been described earlier [20]: $M_N = 50.1 \times 10^3$ g/mol, $M_W/M_N = 1.07$ and $M_N = 81.2 \times 10^3$ g/mol, $M_W/M_N = 1.05$, respectively. We will refer to the deuterated samples as PEP-PEE-2D and PEP-PEE-3D.

PEP-PEE-2 and PEP-PEE-3 exhibit order-disorder transitions at $T_{ODT} = 96$ °C and 291 °C as reported earlier [2]. Deuteration affects this phase transition slightly. Isochronal dynamic mechanical spectroscopy measurements [2, 14] reveal $T_{ODT} = 93$ °C for sample PEP-PEE-2D. We have not measured the order-disorder transition temperature for sample PEP-PEE-3D but can safely assume $T_{ODT} \cong 286$ °C based on the value determined for the hydrogenous material; an error of several degrees in this estimate will not affect the conclusions of this work.

Small-angle neutron scattering (SANS) and rheometry specimens were prepared by compressing the diblock copolymer between two teflon-covered plates that were separated by 1 mm thick shims. This was carried out at 100 °C for PEP-PEE-2D and 200 °C for PEP-PEE-3D while under vacuum ($< 10^{-1}$torr). Following this procedure, the pressed sheets were loaded into a shearing apparatus that we have designed and built for the purpose of studying the effects of large amplitude shearing deformations on block copolymer melts.

The shearing apparatus used in this study was inspired by the device described by Hadziioannou *et al.* [6-8]. It consists of two 5.08 x 5.08 x 0.635 cm parallel brass plates that have been laminated with a thin teflon sheet. The plates are loaded, with the teflon side exposed, into two parallel brass heating blocks that can be independently controlled over the range $25 - 300° \pm 0.1$ °C. When both blocks are heated to the same set point (as was done for all of the experiments of this paper) the temperature measured by a thermocouple within the polymer, after equilibration, is within 0.1 °C of the set point. The top heating block is stationary, but its elevation with respect to the bottom heating block (and thus the gap between

the plates) can be varied through the use of appropriately sized shims. Once the appropriate gap is produced, the top heating block is locked in place by a support structure equipped with a movable locking jaw and the shims are removed. The bottom heating block is mounted on a motorized, screw-driven, dovetail slider that can be operated between 0.0019 – 4.2 mm/s. Two limit switch reversing circuits are mounted on the slider and allow for linear oscillatory motion of the bottom plate with a minimum displacement of 1.0 mm. During operation the apparatus is held inside a sealed chamber that can maintain either a vacuum or a nitrogen gas atmosphere.

Shear oriented block copolymer samples are produced as follows. Preformed sheets of polymer are prepared as mentioned above with a thickness slightly larger than the desired thickness. Next, the teflon covered brass plates are loaded into the heating blocks and the specimen is placed on the bottom plate. Shims are placed on the bottom heating block next to the sample. The top plate (and top heating block) is then rested on the sample. A gap exists between the top heating block and the shims; the polymer specimen supports the weight of the top plate and heating block. The chamber is then sealed and cycled several times between vacuum and nitrogen, and the sample is subsequently heated under a slight over-pressure of nitrogen to a temperature sufficient for it to flow to the desired thickness. After cooling the chamber is opened and the top heating block is locked in place and the shims are removed.

At this point the chamber is again sealed and purged with nitrogen. After heating to the desired temperature, shearing is conducted at a specified strain amplitude and shear rate. Upon completion of the deformation process the apparatus is cooled and the polymer specimen is then removed from the sandwich through the careful use of a razor blade and methanol (as a releasing agent).

All of the polymer specimens sheared in this study were 1 mm thick and each was sheared using a 100 % strain amplitude ($\gamma = 1$) with a total travel length for one complete cycle of 4 mm. Future experiments will probe strain amplitude as a variable. The strain rate of the shear orientation is reported as a frequency ω in order to facilitate comparison with frequencies used in the small strain, dynamic rheological tests; $\omega = 2\pi/t_p$, where t_p is the time period required to complete one cycle, $t_p = 4\gamma/(d\gamma/dt)$. When using a 100 % strain amplitude the frequency and strain rate are related by $\omega = (\pi/2)(d\gamma/dt)$. Shear orientation temperatures and frequencies used in this study are listed in table I. All specimens discussed here were subjected to 15 hours (i.e., 170 to 8600 cycles) of shearing.

Table I. — *Shear orientation processing conditions.*

Polymer Sample	T(°C)	T(K)/T_{ODT}(K)	ω(rad/s)	ω/ω_χ	Lamellae Orientation
PEP – PEE – 2D	83	0.97	0.02	0.0002	parallel
PEP – PEE – 2D	83	0.97	1.0	0.01	perpendicular
PEP – PEE – 3D	150	0.75	1.0	0.02	parallel

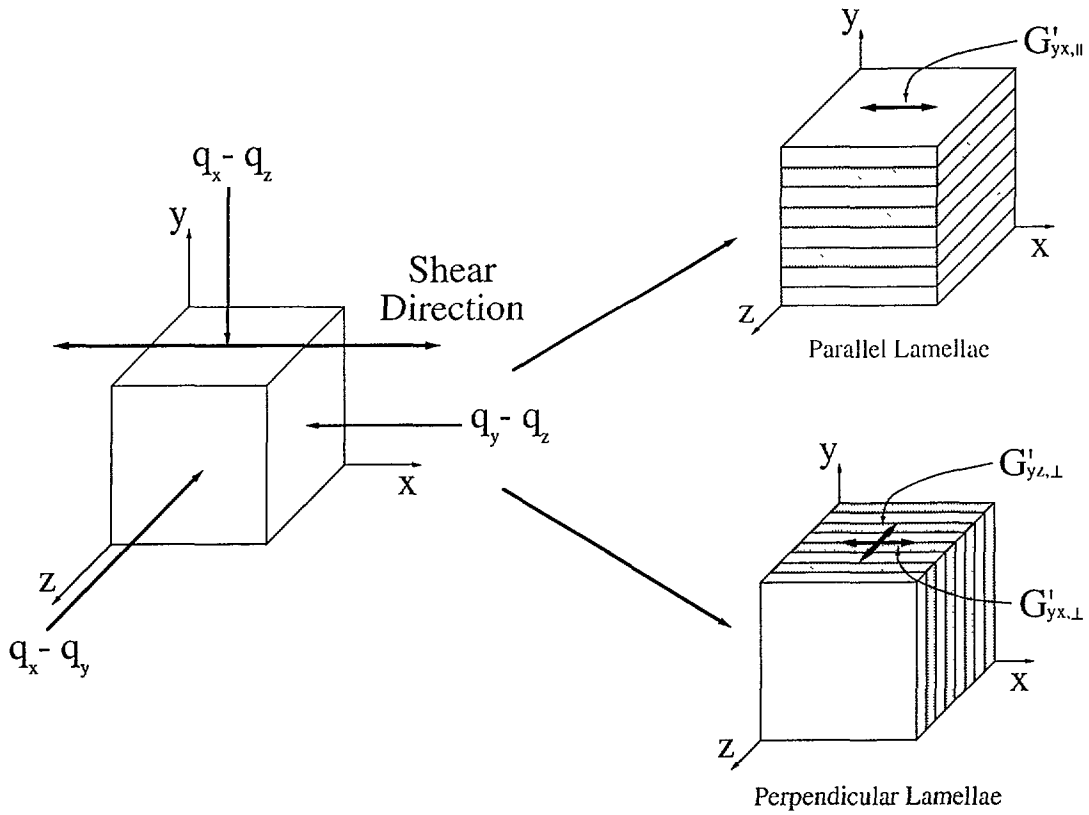

Fig. 1. — Coordinate system for the rheological and SANS experiments. Double-ended arrows indicate dynamic shearing directions for large amplitude processing (left side) and small amplitude dynamic mechanical testing (right side). Single ended arrows (left side) identify the three neutron beam orientations used and the associated scattering planes. Depending upon the shearing frequency and temperature two lamellae orientations, parallel and perpendicular, are obtained with 100 % amplitude dynamic shearing.

Dynamic mechanical measurements were conducted with sheared specimens using a Rheometrics RSAII dynamic mechanical spectrometer operated in a simple shear geometry. Oriented specimens were cut and loaded onto the shear sandwich fixture (1 mm gap) based on the original deformation direction. The dynamic elastic modulus (G') and viscosity ($\eta' = G''/\omega$) were recorded as a function of frequency at 40 °C using a 2 % strain amplitude.

A second series of measurements was conducted on an initially unoriented PEP-PEE-2D specimen. Shear creep compliance and recoverable compliance were measured with a Magnetic Elevation Creep Apparatus (Time-Temperature Instruments, Inc.). This device is a computerized version of the original magnetic bearing torsional creep apparatus of Plazek (21). Parallel circular plates (32 mm in diameter) were used with a gap height of 1.59 mm. After an initial alignment of two or more revolutions, successive experiments creeping in the same direction as the initial alignment always gave reproducible results. All experiments consisted of $5 \times 10^5 - 7 \times 10^5$ seconds of creep followed by a recovery period of at least 10^6 seconds. Both shear compliance and recoverable compliance were found to depend on the level of applied torque, which ranged from 100 to 6500 dyne-cm. Oscillatory shear and steady shear experi-

ments were performed on a Rheometrics RMS-800 Mechanical Spectrometer equipped with a force-rebalanced transducer. Parallel circular plates (25 mm diameter) were used with a gap height of 2.0 mm. The specimens were subjected to two complete revolutions before initiating the dynamic measurements. Oscillatory data were found to depend on strain amplitude, and a 1 % strain amplitude was used for the data reported here. All parallel plate measurements were performed at 30 °C.

SANS specimens were cut from shear oriented sheets, mounted between 0.159 mm quartz windows and sealed with epoxy while under an argon atmosphere. SANS experiments were performed at the Risø National Laboratory located in Roskilde, Denmark, and at the National Institute of Standards and Technology (NIST) situated in Gaithersburg, Maryland. At the former facility $\lambda = 6.0$ Åwavelength neutrons ($\Delta\lambda/\lambda = 0.17$) and a sample-to-detector distance (SDD) of 6 meters was employed. At NIST, $\lambda = 6.0$ Å($\Delta\lambda/\lambda = 0.19$) and a SDD of 10 meters was used. Scattering patterns were recorded on two-dimensional detectors and corrected for background scattering and detector sensitivity. SANS intensities are reported in arbitrary units. Three scattering experiments were performed for each shearing condition, corresponding to the neutron beam incident with each of the three Cartesian coordinates associated with the deformation geometry as illustrated in figure 1.

3. Results and analysis.

3.1 SANS. — Small-angle neutron scattering results obtained from the low ($\omega = 0.02$ rad/s) and high ($\omega = 1.0$ rad/s) frequency dynamically sheared PEP-PEE-2D material ($T = 83$ °C, Tab. I) are presented in figures 2 and 3, respectively. For the low frequency condition strong reflections are evident at scattering wavevectors $\mathbf{q}_y = \pm\, q^* = \pm\, 0.02$ Å^{-1} ($|\mathbf{q}| = 4\pi\lambda^{-1}\sin\theta/2$ where θ is the scattering angle) in the $\mathbf{q}_y - \mathbf{q}_z$ and $\mathbf{q}_y - \mathbf{q}_x$ scattering planes. This result along with higher-order reflections at $\mathbf{q}_y = \pm\, 2q^*, \pm\, 3q^*$ (these are not obvious in the linear intensity scale shown) indicate a lamellar microstructure with unit normal preferentially oriented parallel to the velocity gradient direction (see Fig. 1). We will refer to this orientation as "parallel" lamellae.

The high frequency shearing condition produced a distinctly different result as shown in figure 3. Here, the dominant neutron scattering reflections occur at $\mathbf{q}_z = \pm\, q^* = \pm\, 0.02$ Å^{-1} leading us to conclude that the lamellae have unit normal preferentially oriented perpendicular to both the flow and velocity gradient directions (see Fig. 1). This morphology will be denoted "perpendicular" lamellae. In both cases, the resulting lamellae are not perfect (i.e., truly "single-domain") since there is a discernable ring of scattering at q^* in the $\mathbf{q}_y - \mathbf{q}_z$ scattering plane for the parallel lamellae, and at $\mathbf{q}_y = \pm\, q^*$ in the $\mathbf{q}_x - \mathbf{q}_y$ scattering plane for the perpendicular lamellae. We will return to this point in the discussion section.

In order to assess the stability of the two PEP-PEE-2D lamellar orientations to variations in the shearing frequency we subjected a parallel specimen to the high frequency processing condition, and a perpendicular specimen to low frequency shearing. The SANS results for these experiments revealed that the parallel lamellae transform to the perpendicular orientation during high frequency shearing. However, the perpendicular lamellae retained that orientation when subjected to the low frequency oscillatory deformation. The resulting SANS patterns are not shown since they are very similar to those found in figures 2 and 3. The significance of these observations will become apparent during our discussion of the underlying mechanisms of orientation.

Frequency is not the sole parameter responsible for determining the lamellar orientation in these diblock copolymer melts. Temperature also plays a crucial role, as we illustrate

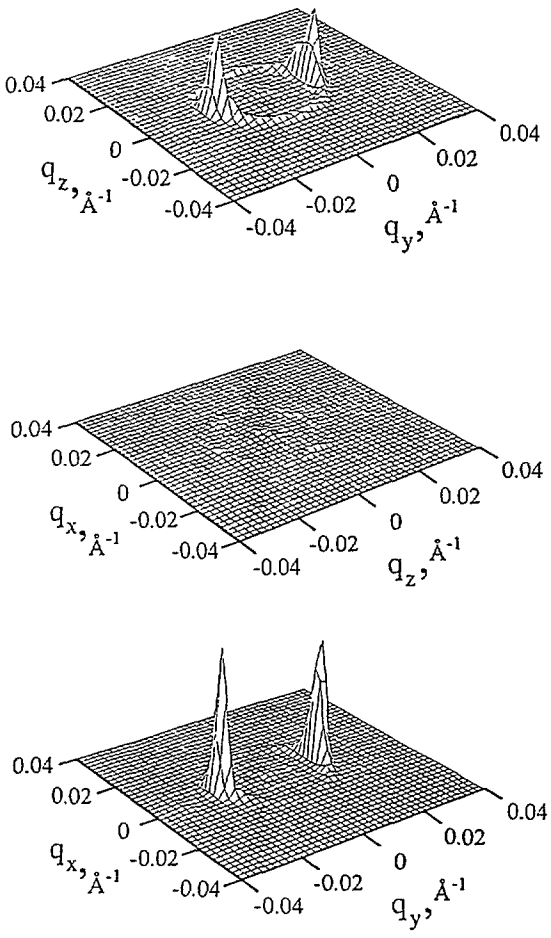

Fig. 2

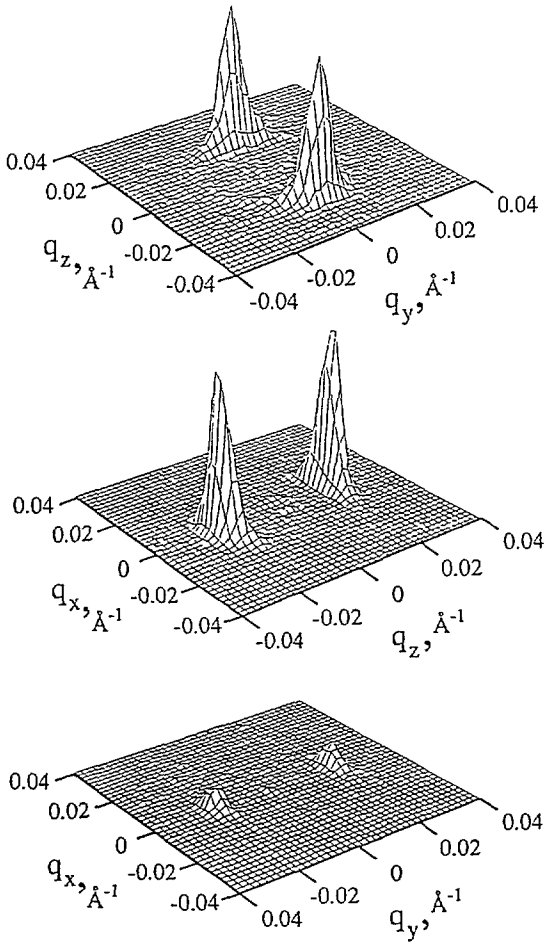

Fig. 3

Fig. 2. — SANS results for sample PEP-PEE-2D following dynamic shearing at $\omega = 0.02$ rad/s ($\omega/\omega_x = 2 \times 10^{-1}$) and $T = 83$ °C ($T/T_{ODT} = 0.97$). These data indicate a parallel lamellae orientation (see Fig. 1).

Fig. 3. — SANS results for sample PEP-PEE-2D following dynamic shearing at $\omega = 1.0$ rad/s ($\omega/\omega_x = 1 \times 10^{-2}$) and $T = 83$ °C ($T/T_{ODT} = 0.97$). These data indicate a perpendicular lamellae orientation (see Fig. 1).

using sample PEP-PEE-3D. This material was sheared at the same high frequency used in producing the perpendicular lamellae in PEP-PEE-2D ($\omega = 1$ rad/s) but at 150 °C. Thus, since $T_{ODT} \cong 286$ °C PEP-PEE-3D was processed much further from the order-disorder transition than was PEP-PEE-2D, $T/T_{ODT} = 0.75$ *versus* 0.97, respectively. However, the effective frequency is actually higher for PEP-PEE-3D due to the significantly higher molecular weight. A convenient reduced reference frequency is the ratio of the shearing frequency to the frequency ω_x where the linear dynamic elastic and loss moduli cross at the low frequency end of the rubbery plateau, $\omega_x = \omega(G'' = G')$; ω_x is approximately the inverse single chain relaxation time [22] in the disordered state. Based on this criterion $\omega/\omega_x = 0.02$ for the high frequency

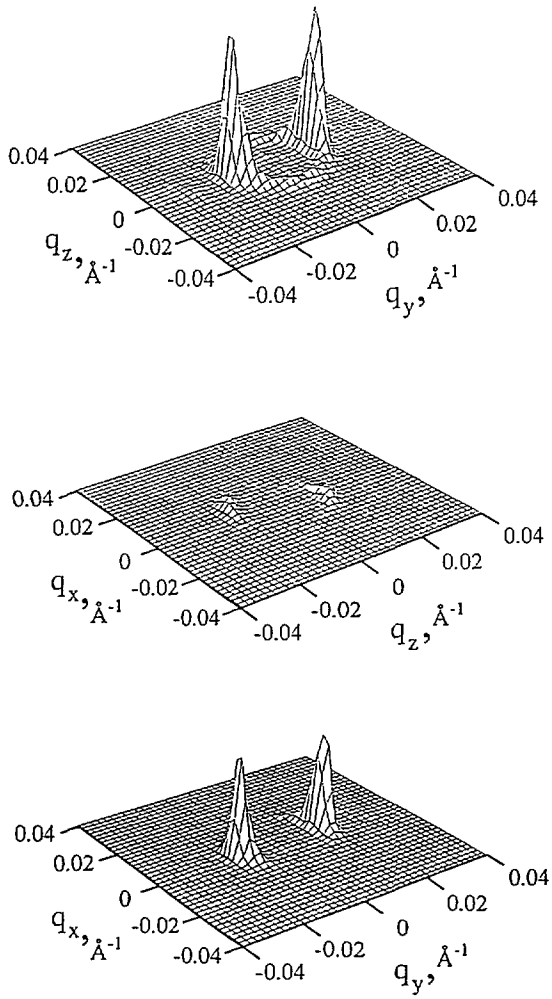

Fig. 4. — SANS results for sample PEP-PEE-3D following dynamic shearing at $\omega = 1.0$ rad/s ($\omega/\omega_x = 2 \times 10^{-2}$) and $T = 150$ °C ($T/T_{ODT} = 0.75$). These data indicate a parallel lamellae orientation (see Fig. 1).

PEP-PEE-3D experiment whereas $\omega/\omega_x = 0.01$ for the corresponding case involving PEP-PEE-2D. Examination of figure 4 reveals that decreasing the reduced temperature T/T_{ODT} has produced a parallel orientation, even at the high relative shearing frequency. As with the PEP-PEE-2D parallel geometry there is a noticeable ring of intensity at q^* in the $\mathbf{q}_y - \mathbf{q}_z$ scattering plane, along with a pair of weak reflections in $\mathbf{q}_x - \mathbf{q}_z$.

3.2 RHEOLOGY. — The effects of shear-orientation are also manifested in the rheological properties of our polyolefin block copolymers. In general five independent shear moduli are required to characterize a lamellar material [23]. For an ideal (i.e., "single domain") incompressible system only three of these will be unique. Using the coordinate system and lamellar orientations given in figure 1 these are: $G_{xy,\perp} = G_{yx,\perp}$, $G_{yz,\perp} = G_{xz,\perp}$, and $G_{zx,\perp} = G_{zy,\perp}$

where the first and second subscripts refer to the direction normal to the shear plane, and the shear direction, respectively [23], and $\perp$ indicates perpendicular lamellae. In the parallel orientation state the corresponding moduli are: $G_{yz,\parallel} = G_{yx,\parallel}$, $G_{xz,\parallel} = G_{zx,\parallel}$, and $G_{zy,\parallel} = G_{xy,\parallel}$. We have determined the dynamic modulus $G^*(\omega) = G'(\omega) + iG''(\omega)$ for PEP-PEE-2D using perpendicular and parallel oriented specimens prepared as described above, where $G'(\omega)$ and $G''(\omega)$ are the dynamic elastic and loss moduli, respectively. The three measurement geometries are illustrated in figure 1, from which $G^*_{yx,\parallel}$, $G^*_{yx,\perp}$, and $G^*_{yz,\perp}$ were obtained. These experiments correspond to deformations with i) the shear plane and direction parallel to the lamellae ($G^*_{yx,\parallel}$), ii) the shear plane perpendicular and the shear direction parallel to the lamellae ($G^*_{yx,\perp}$), and iii) the shear plane and direction perpendicular to the lamellae ($G^*_{yz,\perp}$).

According to figure 1, in principle $G^*_{yz,\parallel} = G^*_{yx,\parallel} = G^*_{zy,\perp} = G^*_{zx,\perp}$ along with analogous relationships for the two other fundamental deformation geometries. In practice, this condition is never exactly satisfied due to the presence of defects and hydrodynamic effects as discussed below. However, the qualitative trends we report are reproduced between the various possible lamellar orientations. A more comprehensive treatment of this issue will be presented in a future communication.

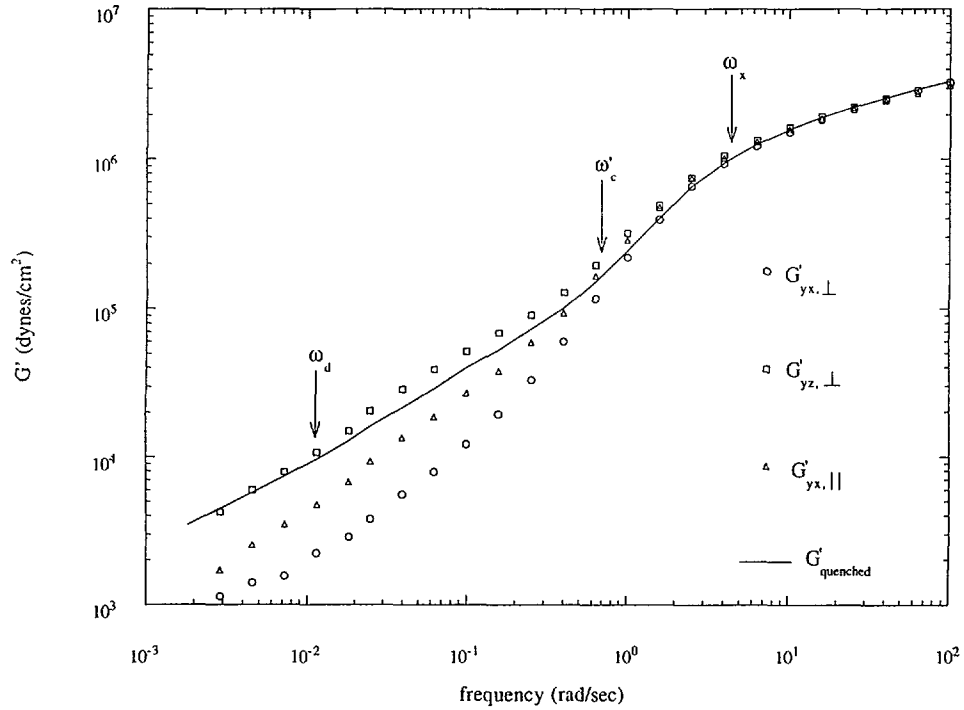

Fig. 5. — Dynamic elastic shear modulus for quenched (solid curve) and dynamically shear-oriented specimens of PEP-PEE-2D (T = 40 °C); shear moduli for the anisotropic specimens are identified relative to the lamellae orientation in figure 1. ω_x is defined by $G'(\omega_x) = G''(\omega_x)$ and is approximately the inverse single-chain longest relaxation (i.e., reptation) time. The viscoelastic properties are dominated by microdomain (lamellar) dynamics when $\omega \lesssim \omega_c$. For $\omega \gtrsim \omega_d$ local (short-range) microdomain properties are probed while collective (long-range) hydrodynamic and defect dynamics are accessed when $\omega \lesssim \omega_d$ (see Fig. 7).

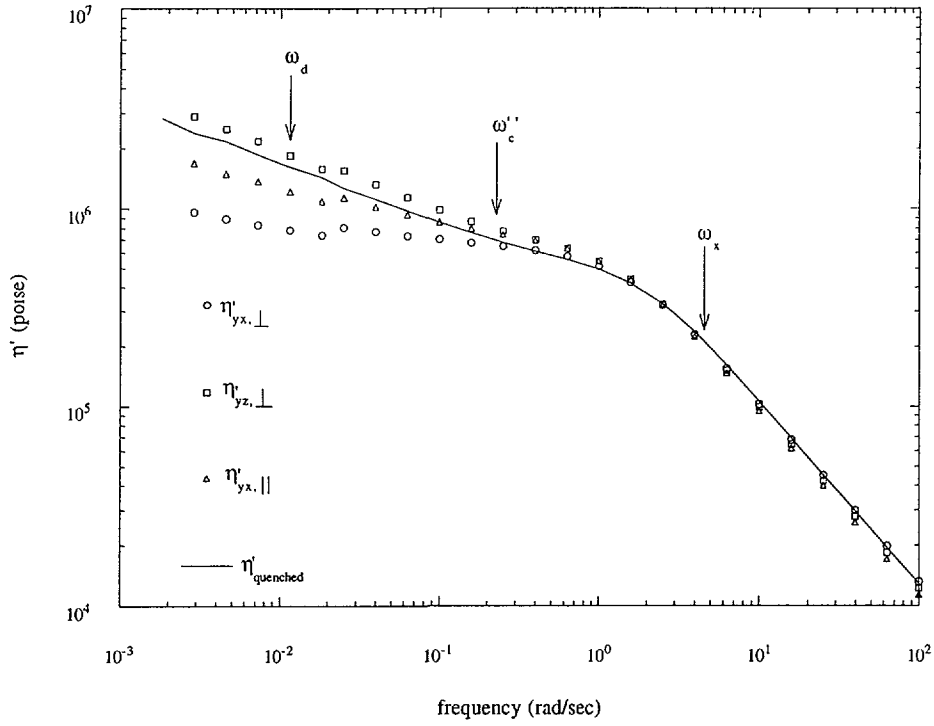

Fig. 6. — Dynamic viscosity ($\eta' = G''/\omega$) for quenched (solid curve) and dynamically shear-oriented PEP-PEE-2D($T = 40$ °C). The characteristic frequencies indicated are as described in figure 5.

The three fundamental dynamic elastic moduli and viscosities ($\eta'(\omega) = G''(\omega)/\omega$) for the oriented PEP-PEE-2D material are presented in figures 5 and 6. Also shown by the solid curves are the responses obtained from this material in the quenched (i.e., unoriented) state [2]. As described in earlier publications [2, 14], these results can be divided into two parts. At frequencies greater than the critical frequency ω_c, $G'(\omega)$ and $G''(\omega)$ (or $\eta'(\omega)$) are thermo-rheologically simple and can be time-temperature superposed. Below ω_c the dynamical properties are controlled by the microdomain structure, and accordingly the time-temperature superposition principle may not be applicable, particularly near the order-disorder transition where the microdomain structure varies significantly with temperature [24]. For the quenched PEP-PEE-2 material $G'(\omega = \omega'_c) \cong G''(\omega = \omega''_c) = 1.5 \times 10^5 \text{dynes/cm}^2$ where $\omega'_c \cong 3\omega''_c$ [2]. These values are identified in figures 5 and 6, along with the crossover frequency $\omega_x \equiv \omega(G' = G'')$.

The shear-oriented PEP-PEE-2D specimens are characterized by anisotropic dynamic mechanical properties for $\omega \lesssim \omega_c$; $G'_{yx,\perp} < G'_{yx,\parallel} < G'_{yz,\perp}$ and $\eta'_{yx,\perp} < \eta'_{yx,\parallel} < \eta'_{yz,\perp}$. We have also observed these trends in a variety of other polyolefin diblock copolymers exhibiting a lamellar morphology. The magnitude of the differences in G' and η' are somewhat dependent on processing conditions, particularly the reduced temperature T/T_{ODT}, but the relative properties found in figures 5 and 6 appear to be general/In several instances $G'_{yx,\perp}$ and $\eta'_{yx,\perp}$ have been reduced to near terminal behavior ($G' \sim \omega^2$ and $\eta' \sim \omega^0$), over a finite frequency range, by our shear-orientation process [16]. These results provide important evidence regarding the relaxation processes that occur when block copolymer lamellae are deformed, and will

contribute to our tentative explanation of the variable shear-induced lamellar orientation.

The greatest resistance to shearing occurs when the unit normal to the lamellae is oriented parallel to the shear direction. Since the material is incompressible this deformation necessitates a tilting and thinning of the lamellae, or a rearrangement of the polymer chains such that the periodicity is preserved while the number of lamellae decreases. The former response requires unfavorable block coil configurations, while the later is kinetically constrained. In the presence of large strains this geometry is unstable and the lamellae reorient (see discussion section).

Intuitively we expected $G'_{yx,\parallel}$ and $\eta'_{yx,\parallel}$ would be *lower* than $G'_{yx,\perp}$ and $\eta'_{yx,\perp}$, but this is *never* observed. In principle, as $\omega \to 0$, an ideal, incompressible specimen (i.e., flat "single-domain" lamellae) should offer no resistance other than intermolecular friction to deformations that force the lamellae to slide by each other. For this to be true the frequency must be sufficiently low such that entanglements have adequate time to relax completely. However, experimentally these materials are never perfect. At finite temperatures there is a thermodynamic lower bound on the number density of defects that increases as the ODT is approached. Furthermore, in this range of temperatures near the ODT, hydrodynamic modes of lamellar movement, such as undulation, peristaltic, baroclinic and second-sound modes [19, 25], will be active. The imposed shear flow might interact with these hydrodynamic modes in ways that depend on the orientation of the lamellae.

At intermediate frequencies ($\omega_d \lesssim \omega \lesssim \omega_c$) a second factor, vorticity ($\nabla \times \mathbf{v}$), may be important. With the shear direction and gradient oriented parallel and perpendicular, respectively, to the lamellae (i.e., the parallel orientation in Fig. 1) vorticity will tend to bend the lamellae [19], which will be opposed by interfacial tension and dynamic factors that tend to rigidify the interface. The result will be an increase in G' and η'. In the perpendicular orientation (i.e., with the shear direction and gradient parallel to the lamellae) vorticity will not couple to the lamellar structure (i.e., the local composition fluctuations) which may also contribute to the explanation of why $G'_{yx,\perp} < G'_{yx,\parallel}$ and $\eta'_{yx,\perp} < \eta'_{yx,\parallel}$ at intermediate frequencies.

Above ω_c, the rheological properties are dominated by relaxation processes intrinsic to unstructured (e.g. homopolymer) melts such as entanglement and glassy modes. Since $\omega_c < \omega_x$ (recall that ω_x is the reciprocal of the longest relaxation time in the disordered state) we expect viscoelastic response in the range $\omega_d \lesssim \omega \lesssim \omega_c$ to be governed by microdomain (i.e., interfacial) deformations. Accordingly, the modulus should be controlled by the specific interfacial area ($\sim d^{-1}$), so that

$$| G^*(\omega_c) | \cong \frac{k_B T}{b^2 d} \sim N^{-\delta} \tag{1}$$

where b is the average monomer size (Kuhn length) d is the lamellar period, and the exponent δ has been experimentally determined to be about $\delta = 4/5$ near the ODT [8, 15]. The magnitude of this modulus is roughly correct, and we test the scaling with N in a separate publication [2] where we show that $G'(\omega'_c, N_1 = 895)/G'(\omega'_c, N_2 = 1890) \cong 2.0$ in close agreement with the ratio $(N_1/N_2)^{-4/5} = 1.8$, which supports the idea that, for $\omega \lesssim \omega_c$, the rheological properties are controlled by the domain structure.

In order to characterize more thoroughly the low frequency behavior of the oriented material we conducted a series of rheological measurements using the parallel plate geometry. (Small-angle X-ray scattering measurements confirmed that a parallel orientation is produced by the revolutions imposed on the material prior to these experiments.) Figure 7 depicts the results of three separate experiments: dynamic shear ($\eta^*(\omega)$), steady shear ($\eta(\dot{\gamma})$), and creep ($\eta(\dot{\gamma})$) where $\dot{\gamma}$ refers to the shear rate. These measurements provide a dynamical fingerprint of PEP-PEE-2 over nine orders-of-magnitude in time, without reliance on the time-temperature superposition technique. The complex viscosity $\eta^*(\omega)$, plotted as open circles in figure 7, is very

similar to that reported in figure 6; note, however, that the frequency scale is shifted slightly since the two measurements were conducted at different temperatures. Apparent viscosities in steady shear at 10^{-3} and $10^{-2}s^{-1}$ are also plotted in figure 7 as filled circles. The empirical Cox-Merz rule [26], equating $\eta^*(\omega)$ with the apparent viscosity at the corresponding shear rate, $\eta^*(\omega = \dot{\gamma}) = \eta(\dot{\gamma})$, appears to hold for PEP-PEE-2 over this limited range of shear rates. Higher shear rates could not be used due to the onset of flow instabilities.

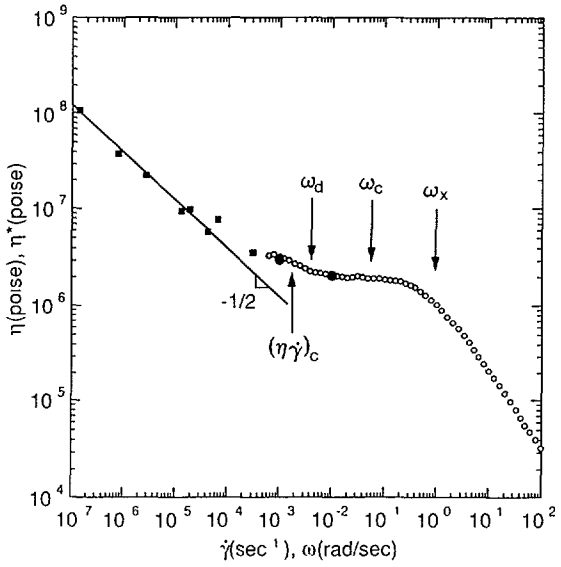

Fig. 7. — Viscosity of sample PEP-PEE-2 (parallel lamellae) obtained at 30 °C using the parallel plate geometry: (o) dynamic, (•) steady shear, and (▪) creep measurements. The characteristic frequencies are as described in figure 5. $(\eta\dot{\gamma})_c$ locates the critical condition for lamellar disorientation as described by equation (4).

The shear rate dependence of apparent viscosity from the creep experiments is shown as filled squares in figure 7 while recoverable compliance is plotted in figure 8 for the torque values indicated (note that the points represent the 100 dyne-cm data). At short times, all torque levels yielded the same recoverable compliance, but at long times the recoverable compliance decreased as torque increased, indicating a non-linear response. At all torque levels, the recoverable compliance continued to increase beyond 10^5s, indicating the presence of longer-time relaxation modes. This observation is consistent with the apparent viscosity not reaching a Newtonian plateau at the lowest shear rates (Fig. 7).

Thus, we have identified three dynamical regimes for PEP-PEE-2D: high, intermediate, and low frequencies, corresponding to $\omega \gtrsim \omega_c$, $\omega_d \lesssim \omega \lesssim \omega_c$, and $\omega \lesssim \omega_d$, respectively. A new characteristic frequency, ω_d, is associated with the crossover from an interfacial (i.e., domain) dominated rheological response to one that reflects ordered state defects such as dislocations and disclinations and hydrodynamic effects associated with undulation, peristaltic, baroclinic and second sound modes. Careful examination of figure 5 reveals evidence of the intermediate regime in the dynamic elastic properties of the shear-oriented material. Most obvious is a "bump" in $G'_{yz,\perp}$ and an upturn in the frequency dependence of $G'_{yx,\perp}$ for $\omega < \omega_d$. In earlier

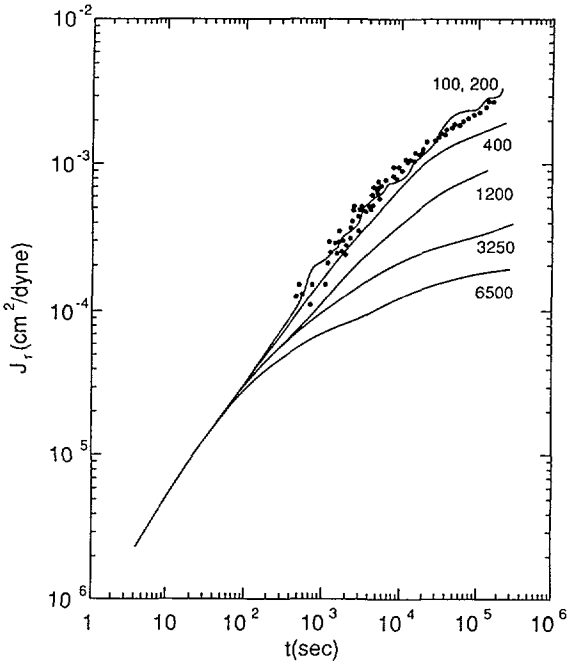

Fig. 8. — Recoverable compliance for PEP-PEE-2 (parallel lamellae) at 30 °C. The curves correspond to the torque levels (dynes-cm) indicated (the points represent a torque of 100 dyne-cm). These results indicate a non-linear response at long times and a longest relaxation time of greater than 3×10^5s.

publications [2, 14] we have shown that near the ODT the disordered melt exhibits a transition to a terminal behavior ($G' \sim \omega^2$) at approximately ω_d. From these observations we conclude that for $\omega_d \lesssim \omega \lesssim \omega_c$ stresses are supported primarily through the domain structure both above and below the order-disorder transition. At this time we cannot distinguish between the effects of defects and hydrodynamics for $\omega \lesssim \omega_d$. However Kawasaki and Onuki (27) attribute the dynamic mechanical properties of quenched specimens [2, 14], $G' \sim G'' \sim \omega^{1/2}$, to overdamped second sound modes; note that we find $\eta' = G''/\omega \sim \omega^{-1/2}$ for $\omega << \omega_d$ (Fig. 7) in a parallel specimen. Presumably defect motion is restricted by the coherent long-range correlations between lamellae in the ordered state. Increasing the temperature above T_{ODT} destroys this constraint thereby eliminating defects, and any low frequency hydrodynamic modes, leading to liquid-like behavior for $\omega \lesssim \omega_d$ [2,14].

4. Discussion.

In the previous section we have documented a frequency and temperature dependence to the lamellar orientation in dynamically sheared symmetric diblock copolymer melts. These results are presented in the reduced form ω/ω_x *versus* χ_{ODT}/χ in figure 9, where $\chi(T)$ has been estimated from T_{ODT}, N, and mean-field theory, $(\chi N)_{ODT} = 10.5$ [28]. Also shown in figure 9 are the results of nine other experiments on PEP-PEE, PEP-PE, and PE-PEE diblock copolymers where PE and PEE signify poly(ethylene) and poly(ethylethylene), respectively. In all cases the materials were dynamically sheared with a 100 % strain amplitude while in a lamellar state; details of these studies will be presented separately [29]. Open and filled

symbols represent parallel and perpendicular lamellar orientations, respectively, as determined by SANS. The points accompanied by a vertical line indicate that additional ordered phases are encountered upon heating from the lamellar state [16]. Since in these cases χ_{ODT} is probably not the appropriate normalization factor the range χ_{ODT}/χ to χ_{LOOT}/χ is given where χ_{LOOT} refers to the order-order transition involving the lamellar state. These data present a coherent picture regarding the parameters that control lamellae orientation. Perpendicular lamellae are obtained for $\omega \gtrsim \omega_d$ as $\chi \to \chi_{ODT}$ while outside this window the parallel orientation is favored. To the best of our knowledge this is the first experimental documentation of the perpendicular orientation in sheared block copolymer lamellar phases.

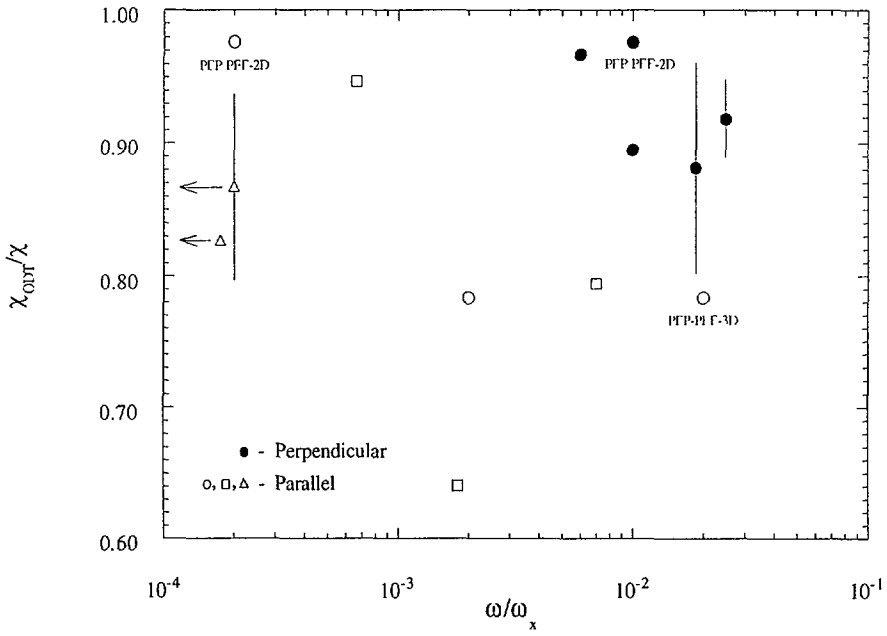

Fig. 9. — Reduced plot of lamellar orientation for various saturated polyolefin diblock copolymers subjected to $\gamma = 100$ % strain amplitude dynamic shearing. Open and filled symbols refer to parallel and perpendicular orientations as defined in figure 1. Symbol notation is: (o), (•) PEP-PEE, (□) PEP-PE, (Δ) PE-PEE. Vertical lines identify the range in χ between the lamellar-order transition and ODT for samples exhibiting multiple ordered phases [16].

In a closely related theoretical study Cates and Milner [30] have shown that increasing the steady shear rate on a mesomorphic material characterized by a lamellar-to-isotropic transition increases T_{ODT} while decreasing $T_{ODT} - T_s$ where T_s is the stability limit for the isotropic state. This occurs through the suppression along the velocity and velocity gradient directions of the non-linear fluctuations of the order parameter that are responsible for the first-order character of the ODT ($T_s \to -\infty$ as $\dot{\gamma} \to 0$) [31, 32], thereby driving the system towards mean-field (i.e., second-order) behavior and a perpendicular orientation. These are the same fluctuations that are responsible for the complex rheological properties just above T_{ODT} [2, 14]. We believe that these disordered state properties are associated with the deformation of a fluctuating structure that can be interpreted as a highly defective, locally ordered microstructure [14]. At

low frequencies ($\omega << \omega_c$) this structure offers no coherent resistance to defect motion and the material is characterized by a Newtonian viscosity. We also believe that the introduction of long-range order ($T < T_{ODT}$) coordinates and retards the movement of defects, and that the ordered lamellae can support certain hydrodynamic modes leading to the properties reported in figures 5 and 6 for $\omega \lesssim \omega_d$. At intermediate frequencies, $\omega_d \lesssim \omega \lesssim \omega_c$, shear stresses are supported by the local interfacial (i.e. domain) structure both above and below the ODT [2, 14]. Here we speculate that the perpendicular orientation derives from the disordering ("melting") of the lamellae with immediate regrowth as predicted by Cates and Milner [30]. Melting occurs because the interfacial material is deformed by the vorticity component of the velocity gradient for all but the perpendicular orientation, as illustrated in figure 10. Distortion and breakup of the parallel and transverse morphologies will ensue provided sufficient stresses are applied to overcome the thermodynamic barriers to disordering. Naturally, these barriers will decrease at $T \rightarrow T_{ODT}$, which would account for our observation that production of perpendicular lamellae only occurs near the ODT.

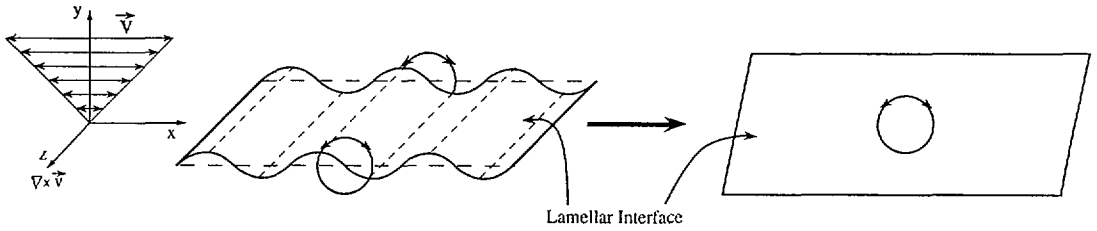

Fig. 10. — Shematic representation of lamellar deformation induced by vorticity ($\nabla \times \vec{v}$) for $\omega \gtrsim \omega_d$. We postulate that as $T \rightarrow T_{ODT}$ this mode of deformation leads to disordering followed by reordering with the lamellar unit normal perpendicular to both the flow and velocity gradient directions, i.e., in the perpendicular orientation.

This mechanism does not account for the development of the parallel orientation for $\omega \lesssim \omega_d$ when $T \rightarrow T_{ODT}$. At these lower frequencies, local interfacial stresses have time to relax, and defects (presumably disclinations and dislocations) and hydrodynamic effects become the dominant stress-bearing structural features. The application of strain will cause defects to move, similar to what occurs in conventional ductile materials above the yield stress. Although we have no direct evidence of the type or number of defects present in our sample, or what mechanism governs their movement, we suspect that the parallel morphology is produced by defect motion. Shearing a "polycrystalline" (e.g., quenched) specimen will focus stresses on those grains that exhibit orientations fully or partly transverse to the plane of shear. Relaxing these stresses requires a reorientation of the microstructure. At low frequencies (or far from the ODT) the barrier to melting (i.e., disordering) individual grains will be insurmountable, just as coherent slip in simple crystals is not possible using stresses below the theoretical strength. However, by breaking and reforming the lamellae individually, through the movement of dislocations (or disclinations) lamellar reorientation may be facilitated with the result as sketched in figure 11. Presumably the greatest resolved stress occurs for defects that travel in the shear direction and parallel to the plane of shear, based on the resulting lamellar orientation.

In support of this mechanism we make the following observations. If our speculation regarding maximum resolved stress on the defects in the parallel geometry is correct, then in the perpendicular mode there should be no resolved stress. Our inability to reorient the perpendicular lamellae with low frequency shearing is consistent with this deduction. (It may also

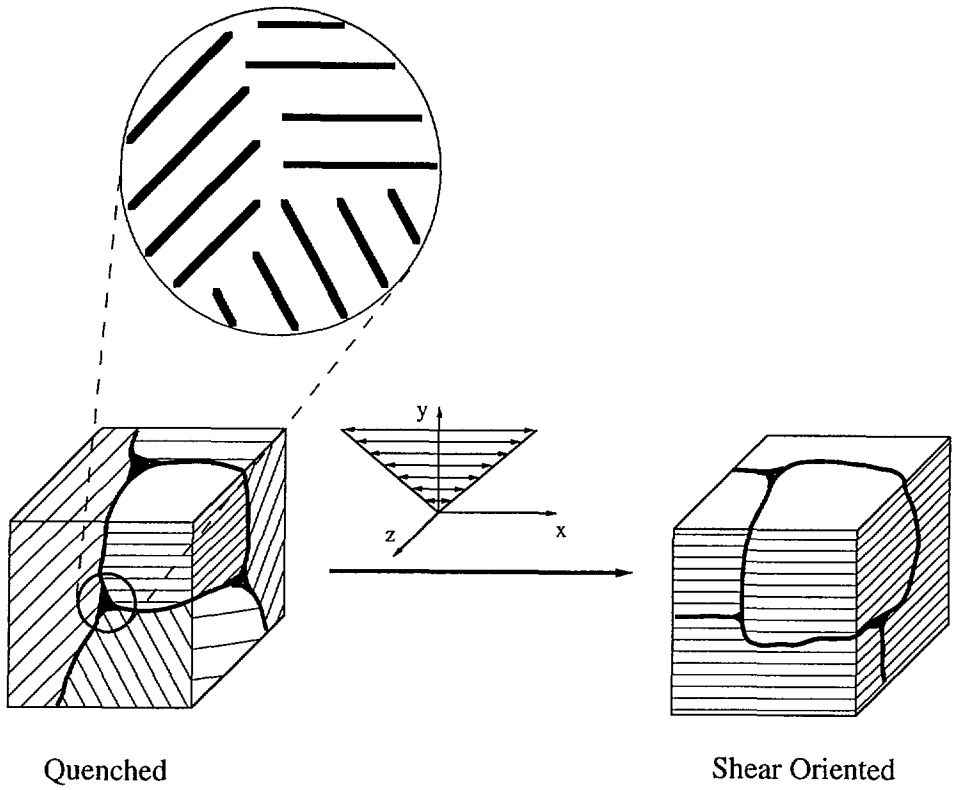

Fig. 11. — Production of the parallel lamellae orientation is speculated to be mediated by the movement of defects, such as those associated with grain boundaries.

be that the perpendicular orientation is the most stable one at any shear rate but cannot be reached unless the shear stress exceeds some threshold level.) This may also account for the low intensity ring of scattering at q^* obtained in the $\mathbf{q}_y - \mathbf{q}_z$ scattering plane for the parallel orientation (see Figs. 2 and 4). If the defect mediated mechanism does not influence grains oriented parallel to the shear direction (regardless of orientation with respect to the shear plane) then the subset of grains initially aligned in this way will be present following the orientation process, leading to a low intensity of scattering at all $q*$.

The feasibility of defect mediated reorientation might also be questioned based on the barriers to locally breaking and reforming lamellae well below the ODT. Our recent discovery [16] of order-order phase transitions (OOT's) in diblock copolymer melts as much as 100 °C below T_{ODT} demonstrates the fascile nature of such microstructural rearrangements, and supports the feasibility of what we propose.

Finally, these findings appear to be closely related to several recent developments involving sheared liquid crystalline lamellar phases. Safinya *et al.* [12] describe an intriguing shear-rate dependence of the nematic director near the nematic-smectic A transition temperature, T_{NA}, of a thermotropic liquid crystalline material. In the smectic A phase a perpendicular orientation is reported above a critical shear rate $\dot{\gamma}_c$ that increases with decreasing temperature, while below $\dot{\gamma}_c$, a mixed parallel and perpendicular arrangement is obtained. This is remarkably similar to what we show in figure 9. [Note that we are attributing the perpendicular orientation in the

block-copolymers to the Cates-Milner [30] mechanism which is not strictly applicable to the smectic A-nematic transition.]

There exists another recent related theoretical development [19]. When the shear-rate approaches the reciprocal of the microstructural relaxation time, $\dot{\gamma}\tau \approx 1$, the structure of a mesomorphic material will be distorted. We can estimate τ as the time it takes for a copolymer chain to diffuse a distance equal to its coil size. According to Fetters [33], the characteristic ratio [34] of PEP is $C_\infty = 6.7$ and for PEE, $C_\infty = 5.7$. From this we estimate the end-to-end distance of PEP-PEE-2 to be R = 180 Å (as a random coil, above T_{ODT}). Shull *et al.* [35] report a self-diffusion coefficient $D \cong 1 \times 10^{-14}$cm^2/s at 30 °C for PEP-PEE-2. Thus, the relaxation time $\tau \cong R^2/D \cong 300$ s for PEP-PEE-2 at 30 °C, which agrees rather well with $\omega_d \cong 4 \times 10^{-3}$ rad/s. We therefore speculate that

$$\omega_d \cong \frac{1}{\tau} \cong \frac{D}{R^2} \tag{2}$$

where D is the diffusion coefficient of the copolymers for motion along their lamellae. The modulus at frequency ω_d is apparently determined by the interlamellar spacing,

$$| G^*(\omega_d) | \cong \frac{k_B T}{d^3} \tag{3}$$

For $\dot{\gamma}\tau \lesssim 1$, viscous or dissipative forces dominate while elastic deformations result when $\dot{\gamma}\tau \gtrsim 1$. A theoretical treatment of the effects of shear-flow on lamellar liquid crystals by Bruinsma and Rabin [19] yields,

$$(\eta\dot{\gamma})_c \simeq \frac{(k_B T)^{5/2}}{K^{3/2} d^3} \tag{4}$$

where $(\eta\dot{\gamma})_c$ is the critical stress for layer collapse (i.e., disorientation), K represents the lamellar binding energy, and d is the interlayer spacing. Since our experiments were done near T_{ODT} we will assume $K \sim k_B T$, which together with $d = 300$ Å [24] gives $(\eta\dot{\gamma})_c \sim 2 \times 10^3$ dynes-cm^{-2}. Examination of figure 8 reveals that $\dot{\gamma}_c \approx \omega_d$ as expected since with $K = k_B T$, and the apparent validity of the Cox-Merz rule, equation (3) follows from equation (4).

Thus, certain aspects of sheared smectic liquid crystals appear to be strikingly similar to dynamically sheared block copolymer melts when $\dot{\gamma}\tau \gtrsim 1$ (or $\omega \gtrsim \omega_d$). However, we suspect that this analogy will break down when $\dot{\gamma}\tau << 1$ (or $\omega << \omega_d$). Here, block copolymer orientation appears to be mediated by low energy defects that are difficult if not impossible to remove from the material. Conversely, defects are readily expelled from smectic A thermotropics. This observation is consistent with the efficient production of parallel lamellae in block copolymers at low-shearing frequencies while a mixture of orientations are obtained from the smectic A material at low shear rates [12].

5. Summary.

We have shown by small angle neutron scattering that two orientations can be generated when diblock copolymer lamellae are subjected to a large amplitude (100 %) oscillatory shearing deformation. At high frequencies, $\omega \gtrsim \omega_d$ and near the order-disorder transition, $T \rightarrow T_{ODT}$, the resulting morphology has lamellae oriented perpendicular to the shear plane and coincident with the shear direction. Outside this processing window, $\omega \lesssim \omega_d$ and $T << T_{ODT}$, the lamellae are arranged parallel to the plane of shear. Two distinct mechanisms are proposed to account for these findings. The high frequency behavior near the ODT is attributed to

the melting and regrowth of the microstructure where the effect of vorticity leads to the suppression of all but the perpendicular lamellar arrangement. Away from the ODT, and at low frequencies, defect motion is believed to be responsible for producing the parallel morphology. These speculations are supported by rheological measurements that document the anisotropic viscoelastic properties of the oriented material. Below ω_d the rheological behavior appears to be governed by the presence of defects and/or hydrodynamic effects, for $\omega_d \lesssim \omega \lesssim \omega_x$ the dynamic mechanical response is dominated by the local microdomain (i.e., interfacial) structure, while above ω_x the response is controlled by entanglements.

Acknowledgements.

Support for this research was provided by the United States Air Force Office of Scientific Research (AFOSR-90-0207) and the Center for Interfacial Engineering (CIE), a National Science Foundation Engineering Research Center at the University of Minnesota. Additional support has been provided to KA by the Danish Programme for Materials Technology. Jeffrey Rosedale and Ian Hamley are acknowledged for enlightening discussions, along with Julie Kornfield who also carefully reviewed the manuscript.

References

[1] Bates F.S. and Fredrickson G.H., *Ann. Rev. Phys. Chem* **41** (1990) 525.
[2] Rosedale J.H. and Bates F.S., *Macromolecules* **23** (1990) 2329.
[3] Keller A., Pedemonte E. and Willmouth F.M., *Kolloid-Z.Z. Polym* **238** (1970) 25; *Nature* **225** (1970) 538.
[4] Keller A. and Odell J.A., in Processing Structure and Properties of Block Copolymers, Folkes M.J., Ed., (Applied Sci., 1985) p.29.
[5] Terrisse J., Thesis (1973) Université Louis Pasteur de Strasbourg.
[6] Hadziioannou G., Mathis A. and Skoulios A., *Colloid Polym. Sci.* **257** (1979) 136.
[7] Hadziioannou G. and Skoulios A., *Makromol. Chem., Rapid Commun.* **1** (1980) 693.
[8] Hadziioannou G., Picot C., Skoulios A., Ionescu M.-L., Mathis A., Duplessix R., Gallot Y. and Lingelser J.-P., *Macromolecules* **15** (1982) 263.
[9] Ackerson B.J., Hayter J.B., Clark N.A. and Cotter L., *J. Chem. Phys.* **84** (1986) 2344.
[10] Stevens M.J., Robbins M.O. and Belak J.F., *Phys. Rev. Lett.***66** (1991) 3004.
[11] Penfold J., Staples E. and Cummins P.G., *Adv. Colloid Interface Sci.* **34** (1991) 451.
[12] Safinya C.R., Sirota E.B. and Plano R.J., *Phys. Rev. Lett.***66** (1991) 1986.
[13] Morrison F.A., Winter H.H., Gronski W. and Barnes J.D., *Macromolecules* **23** (1990) 4200; Morrison F.A. and Winter H.H., *ibid* **22** (1989) 3533.
[14] Bates F.S., Rosedale J.H. and Fredrickson G.H., *J. Chem. Phys.***92** (1990) 6255.
[15] Almdal K., Rosedale J.H., Bates F.S., Wignall G.D. and Fredrickson G.H., *Phys. Rev. Lett.***65** (1990) 1112.
[16] Almdal K., Koppi K.A., Bates F.S. and Mortensen K., *Macromolecules* **25** (1992) 1743.
[17] Almdal K., Bates F.S. and Mortensen K., *J. Chem. Phys.* **96** (1992) 9122.
[18] Bates F.S., Rosedale J.H., Fredrickson G.H. and Glinka C.J., *Phys. Rev. Lett.***61** (1988) 2229.
[19] Bruinsma R. and Rabin Y., *Phys. Rev. A* **45** (1992) 994.
[20] Bates F.S., Rosedale J.H., Bair H.E. and Russell T.P., *Macromolecules* **22** (1989) 2557.
[21] Plazek D.J., *J. Polym. Sci. A-2* **6** (1968) 621.
[22] Ferry J.D., Viscolastic Properties of Polymers 3rd Ed. (Wiley, 1980).
[23] Martin P.C., Parodi O. and Pershan P.S., *Phys. Rev. A* **6** (1972) 2401.

[24] Foster M.D., Sikka M., Singh N., Bates F.S., Satija S.K. and Majkrzak C.F., *J. Chem. Phys.* **96** (1992) 8605.
[25] Nallet F., Roux D. and Prost J., *J. Phys. France* **50** (1989) 3147.
[26] Bird R.B., Armstrong R.C. and Hassager O., Dynamics of Polymeric Liquids, Vol.**1** (Wiley, 1977).
[27] Kawasaki K and Onuki A., *Phys. Rev. A* **42** (1990) 3664.
[28] Leibler L., *Macromolecules* **13** (1980) 1602.
[29] SANS and rheological results for the PEP-PE diblock copolymers, will be published by J.H. Rosedale, K. Almdal, K. Mortensen and F.S. Bates, while the PE-PEE system will be reported by J.H. Rosedale, K. Almdal, K. Mortensen, M. Schulz and F.S. Bates.
[30] Cates M.E. and Milner S.T., *Phys. Rev. Lett* **62** (1989) 1856.
[31] Brazovskii S., Zh. Eksp. Teor. Fiz. **68** (1975) 175 [*Sov. Phys.JETP* **41** (1975) 85].
[32] Fredrickson G. and Helfand E., *J. Chem. Phys.* **87** (1987) 697.
[33] Fetters L.J., private communication (1991).
[34] Flory P.J., Statistical Mechanics of Chain Molecules (Hanser, 1989).
[35] Shull K.R., Kramer E.J., Bates F.S. and Rosedale J.H., *Macromolecules* **24** (1991) 1383.